Frontiers of Physics
https://doi.org/10.1007/s11467-020-0951-y
Front. Phys.
15(2), 22602 (2020)

RESEARCH ARTICLE

Light-induced frequency shifts for the lowest vibrational levels of ultracold Cs_2 in the molecular pure long-range 0_g^- state

Ji-Zhou Wu[1,2], Yu-Qing Li[1,2], Wen-Liang Liu[1,2], Jie Ma[1,2,3,†], Lian-Tuan Xiao[1,2], Suo-Tang Jia[1,2]

[1] *State Key Laboratory of Quantum Optics and Quantum Optics Devices, Institute of Laser Spectroscopy, Shanxi University, Taiyuan 030006, China*
[2] *Collaborative Innovation Center of Extreme Optics, Shanxi University, Taiyuan 030006, China*
[3] *College of Physics and Electronic Engineering, Shanxi University, Taiyuan 030006, China*
Corresponding author. E-mail: †mj@sxu.edu.cn
Received September 3, 2019; accepted December 26, 2019

The light-induced frequency shift (LIFS) of ultracold molecular ro-vibrational levels originates from the strong coupling of the atomic-scattering state and the bound-molecular state. In this paper, we present our experimental determination of the LIFSs of the lowest vibrational levels ($\nu = 0$, 1) in the purely long-range 0_g^- state of ultracold cesium molecules. A high-resolution double photoassociation spectroscopy is developed, which serves as frequency ruler to measure the frequency shifts of the lowest molecular levels for Cs_2. The experimental results are qualitatively consistent with the theoretical expectations.

Keywords light-induced frequency shift, ultracold molecule, double photoassociation spectroscopy, long-range state

1 Introduction

Atoms refrigerated to ultralow temperatures (usually < 1 μK) have provided various opportunities in fundamental physics and quantum science [1, 2]. Compared with atoms, molecules are often rich with complex energy-level structures due to their vibrational and rotational degrees of freedom, which present a challenge with respect to implementing sophisticated laser-cooling technologies [3]. Controlling these aspects will open up new possibilities to explore the collective phenomena in quantum many-body systems [4], as well as to synthesize exotic quantum matter with superconductive phases or topological orders [5, 6]. After years of research, ultracold molecules have been successfully produced and manipulated by photoassociation (PA) [7], Feshbach resonances [8], stimulated Raman adiabatic passage [9], and laser cooling [10]. Related research has shown wide applications in cold-reaction chemistry [11, 12], precision measurements [13], quantum simulation [5, 14], and quantum-information processing [15].

As a powerful and versatile approach, the PA of cold atoms has been widely used to produce tightly bound cold molecules [16]. High-resolution PA spectroscopy (PAS) ensures the detailed information of molecule structure, especially for the molecular long-range state. Due to the rich spectra with many different transition types, high-sensitive molecular PAS has been widely used for various atomic species as well as different mixed species [17] to obtain precise molecular parameters [18], to test the stability of fundamental constants [19], and to predict unexplored levels and thus obtain the potential energy curve [20].

Recently, there has been renewed interest in the light-induced frequency shift (LIFS) of the ro-vibrational levels of ultracold molecules formed by PA [21]. The LIFS originates from the light-induced coupling of the atomic-scattering state and the bound-molecular state. The LIFS is crucial and it must be considered when preparing and precisely manipulating ultracold molecular quantum states [22], as well as when measuring the s-wave scattering length [23] and in controlling the interactions between ultracold atoms [24]. Several atomic species have been investigated experimentally on the frequency shift of PA light-induced transitions [21, 25–28]. Moreover, various theoretical models have also been proposed for LIFS based on multichannel-scattering theory [29]. Controlling the LIFS of ultracold Cs_2 ro-vibrational levels based on an external magnetic field has been recently reported by [30]. The LIFSs for molecular hyperfine levels of ultracold polar molecules have also been observed by [31]. Unfortunately, these studies mainly concentrate on the high-lying molecular levels for both homonuclear and heteronuclear molecules. In other words, LIFS studies are yet to examine low-lying molecular levels due to the extremely low probability of PA transition and the suppressed PAS resolution [32]. Specifically, the LIFSs for the lowest vibra-

tional levels in the external well of ultracold Cs_2 molecules — i.e., the pure long range (PLR) 0_g^- state, which usually serves as the intermediate state in transferring the excited molecules to the ground states — are yet to be examined.

In this paper, we develop a robust technique — the double PAS (DPAS) — to measure frequency, demonstrating with high accuracy the LIFS for the lowest vibrational levels ($\nu = 0$ and 1) in the Cs_2 molecular PLR 0_g^- state below the dissociation limit ($6S_{1/2} + 6P_{3/2}$). Accordingly, the linear dependence of the LIFS on PA laser intensity is demonstrated. It should be noted that there have been reports of the missing levels in Cs_2 molecular 0_g^- potential in theory by Bouloufa *et al.* [33] and in experiment [34] that was performed by our group. In order to be consistent with the work that we demonstrated in Refs. [35, 36], here the "lowest levels" are labelled according to the references [17, 18, 35–38]. Indeed, our results provide a groundwork for future works examining the potential curve of the long-range state as well as determining the energy required to prepare stable molecules at ground states.

2 Experiments

Our experimental setup is similar to the one presented by [35]. The experimental scheme is demonstrated in Fig. 1. Ultracold cesium atoms were confined in a typical vapor cell loaded magneto-optical trap (MOT). The trapping laser and the repumping laser were provided by two diode laser systems (Toptica, DL Pro, ~ 100 mW), the frequency drifts of which were narrowed to ~ 0.5 MHz using standard saturated-absorption technology. A quadrupole magnetic field for the MOT was generated using a pair of anti-Helmholtz coils with a typical gradient of 15 Gauss/cm. The measured atomic number was $\sim 4.5 \times 10^7$, which was obtained using the absorption method, and the dimension of the atomic cloud was ~ 800 μm, yielding a peak density with an order of 10^{11} cm^{-3}. The temperature was ~ 150 μK, which was obtained using the time-of-flight method. The cesium atomic fluorescence was collected using a convex lens and detected with a silicon avalanche photodiode (Hamamatsu S3884) with several 850 nm band-pass filters. PA was induced by a widely tunable continuous-wave Ti: sapphire laser (Coherent MBR-110, line width ~ 0.1 MHz, ~ 1 W) pumped by a 10 W Verdi laser. The long-time frequency drift of the Ti: sapphire laser system was less than 500 kHz by locking to its self-reference cavity. The absolute PA laser-frequency measurement was conducted and monitored using a wavelength meter (HighFinesse-Angstrom WS/7R, absolute accuracy ~ 60 MHz), which was calibrated according to the cesium atomic hyperfine resonance transition, $6S_{1/2}$ (F = 4) → $6P_{3/2}$ (F′ = 5), corresponding to a wavenumber of 11 732.176 cm^{-1}.

The production of ultracold molecules by PA is schematically depicted in Fig. 1(a). Two colliding Cs atoms in the $6S_{1/2}$ ground state pair-wisely formed an electronically excited bound molecule by resonantly absorbing a photon from the PA laser with a frequency of ν. The excited molecule de-excited spontaneously into two free atoms or stable ground state molecules. PAS below the dissociation

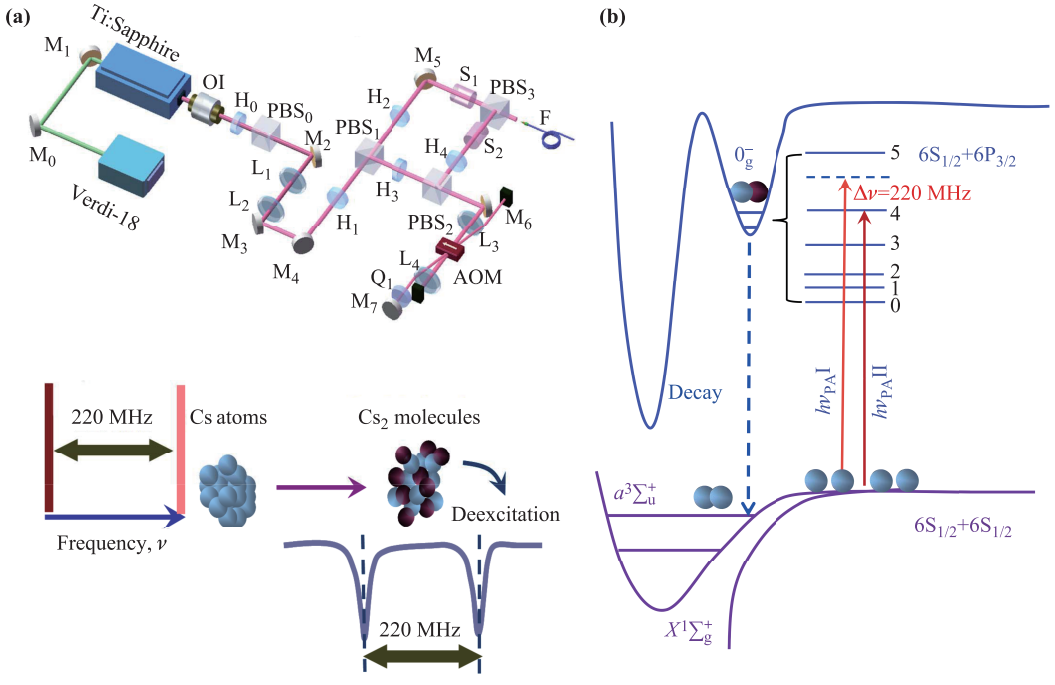

Fig. 1 Experimental schemes. **(a)** Schematic diagram of the double PAS. Experimental setup for the double PA light: optical isolator (OI), half-wave plate (H), quarter-wave plate (Q), polarization beam splitter (PBS), acousto-optic modulator (AOM), mirror (M), lens (L), fiber (F), and shutter (S). **(b)** The related energy levels. Schematic diagram of the PA process and the double PAS.

limit ($6S_{1/2}$ + $6P_{3/2}$, $6P_{1/2}$) was recorded by monitoring the atomic fluorescence with PA laser scans [37, 39]. In this sense, the PAS directly illustrates the produced molecule number as a function of ν.

In order to determine the LIFS, we used a DPAS technique, which provides accurate references to measure the frequency intervals of neighboring rotational levels for the lowest vibrational states. As shown in Fig. 1(b), by alternately controlling the interacting time between the two PA laser beams (I and II) and the MOT, a typical double PA spectrum was recorded. Beam II (i.e., the partial output of the PA laser) was frequency shifted and double passed by an AOM system (MT110-B50A1-IR AA Optoelectronic). As a calibration beam, Beam II had a fixed offset of $\Delta\nu = \nu_I - \nu_{II} = 220$ MHz (the central frequency for the AOM was set as 110 MHz) against Beam I, which was the main output of the PA laser. The two beams were effectively superimposed in space. A typical ro-vibrational PA spectrum including $J = 0, \ldots, n$ (e.g., $n = 4$) was obtained due to the trap loss induced by Beam I. Thereafter, Beam I was switched off and Beam II was switched on to simultaneously interact with the MOT. The time for switching each beam was comparatively shorter ($\sim$ 5 ms) than the loading time ($\sim$ 10 s), in which the resonance peaks are clearly demonstrated with a high resolution without affecting each other. A selected spectral feature containing a resonant rotational level $J = 4$ was scanned twice, and the second resonant peak was labelled as $J' = 4$ in the same spectrum.

In our scheme, the PA laser frequency must be scanned with a high linearity. Accordingly, the frequency was monitored and manipulated in real time using a wavelength meter (WS/7R). The frequency interval between $J = 4$ and $J' = 4$ was exactly equal to 220 MHz. This fixed frequency offset between Beam I and II was used to calibrate the double PA spectra. Accordingly, frequency intervals $\Delta\nu_J$ ($J = 0, \ldots, n-1$) between the neighboring rotational levels were accurately deduced, thereby obtaining the LIFSs.

3 Results and discussion

A lock-in method based on modulating the fluorescence of the ultracold atoms was employed to improve the sensitivity of trap-loss detection. The technique was realized by changing the frequency detuning of the trapping laser. Figure 2(a) depicts the noise-power spectra of the atomic fluorescence as a function of electronic noise of the detection system, comparing the modulation signal and the corresponding higher order terms. From Fig. 2(a), it is evident that the demodulated signal, ω, in the first order (the cyan curve in the inset) corresponds to an optimal signal-to-noise ratio (SNR) of 21, which is much larger than the second and third orders. Therefore, first-order ω is taken as the demodulation-reference frequency.

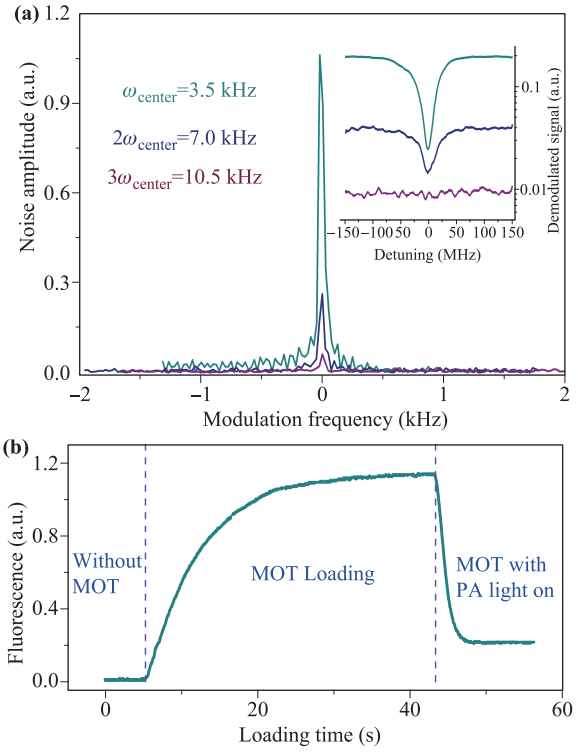

Fig. 2 **(a)** Noise-power spectra of cold atomic fluorescence versus electronic noise of detection system (the inset shows the demodulation signals with the different orders of the demodulation frequency). **(b)** Time evolution of atomic fluorescence with turning the PA laser on and off when MOT is working.

In PA experiments, the response time of the MOT is typically slow ($\sim$ 1 s). Figure 2(b) shows the atomic fluorescence variation as MOT loading as well as with the PA laser on, from which it is evident that the characteristic time is 6.76 s and 1.25 s, respectively. As a result, the PA laser scanning is required slowly to obtain a high-resolution rotational spectroscopy. The PA laser was slowly scanned at a rate of 1 MHz/s.

High-resolution spectra of the low-lying vibrational levels $\nu = 1$ and 0 of the Cs_2 PLR state 0_g^- ($6S_{1/2}$ + $6P_{3/2}$) are shown in Fig. 3, which are red detuned from the ($6S_{1/2}$ + $6P_{3/2}$) dissociation limit for approximately 75.4 and 77.1 cm^{-1}, respectively. The spectrum for the high-lying vibrational level, $\nu = 17$, which is red detuned for 51.0 cm^{-1} from the same dissociation limit, is also shown in Fig. 3 to show the distinctions between PLR states.

DPAS was used to acquire the LIFS values for the aforementioned low-lying vibrational levels, as shown in Fig. 3. At first, the Cs MOT was illuminated by Beam I with an intensity of 102.5 W/cm^2 and $J = 1$–4 rotational levels. Parts of the spectrum containing rotational level $J = 4$ were scanned twice (denoted as $J' = 4$) by Beam II with a fixed frequency difference ($\Delta\nu$) and same laser intensity as Beam I. As $\Delta\nu$ can be set through the AOM, the frequency interval of the neighboring rotational levels, $\Delta\nu_J$, can be directly measured. Compared with the

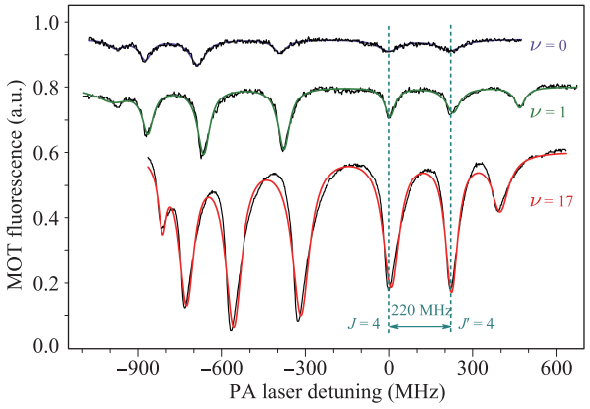

Fig. 3 Typical high resolution DPAS for low-lying vibrational levels $\nu = 0$ and 1 of the Cs_2 0_g^- PLR state. The intensity of beam I and II are both 102.5 W/cm^2. The case for a high-lying vibrational level $\nu = 17$ is also provided for comparison. The colorful curves are the multi–eak Lorentzian fits of the spectra.

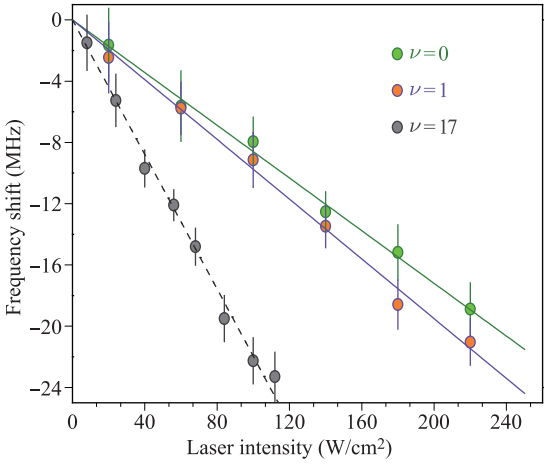

Fig. 4 LIFS values of the PA resonance as a function of PA laser intensity for $\nu = 0$ and 1 of the Cs_2 0_g^- PLR state. LIFS for $\nu = 17$ case is also present for comparison. Colorful circles denote experimental data and the solid lines denote linear fits.

high-lying vibrational levels for the same state [18], $\Delta\nu_J$ for $\nu = 0$ and 1 ranges from 200–450 MHz. The undulation of the spectra for different J values is the result of different Franck–Condon factors (FCF) for the PA transitions between the initial atomic-scattering state and the final ro-vibrational levels of excited molecules.

As the FCF for the lowest level $\nu = 0$ is two orders smaller than $\nu = 17$ for Cs_2 0_g^- state [32, 36], the experimental parameters are optimized to obtain the PA spectra with a high resolution. Hence, the PA laser-scanning rate should be given a small value; namely, 1 MHz/s. The interaction between the PA laser and the cold atomic sample is well performed. Due to the low sensitivity in detecting the signal using long integration times (1 s) of the lock-in amplifier, the PA spectra for $\nu = 0$ can be observed with a low resolution and low reliability [36]. By increasing the integration time to 300 ms, the developed PA spectra are obtained with an improved resolvability. More importantly, by using a DPAS technique, a higher progression $J = 4$ can be acquired, by virtue of which the binding energies of the rotational levels for $\nu = 0$ and the rotational constants can be accurately determined [35]. To be sure, the spectrum for $J = 5$ of $\nu = 0$ is more difficult to acquire than that of $\nu = 1$ and $\nu = 17$. The large rotational progressions can be rationalized due to additional angular-momentum contributions, such as orbital angular momentum due to p-waves or d-waves [18].

By using the DPAS, we are able to accurately measure the LIFS for the lowest vibrational levels, as shown in Fig. 4. For Beam I and II, a given rotational line appears twice in the spectrum with a frequency separation equal to the frequency shift between both beams. Consequently, the frequency interval between the two peak positions is exactly 220 MHz, which serves as an accurate optical-frequency ruler. For beams with unequal intensity, the frequency separation differs from the frequency shifts between both beams. Thus, DPAS allows us to determine the differential light shift.

In Fig. 4, the $\nu = 17$ case is also plotted for comparison with $\nu = 1$ and 0, from which it is evident that the lines become gradually steeper as the quantum number v increases. The slopes for $\nu = 0$, 1, and 17 are -0.086, -0.098, and -0.220 MHz·cm^2/W, respectively. The LIFS effect is pronounced approximal to the molecular-dissociation limit. The error bars mainly originate from the systematic uncertainty in determining beam intensity, which stems from the difficulty associated with accurately measuring the beam diameter at the MOT location. In addition, the interaction between the two laser beams with the MOT, the calibration of the laser-power meter, and the nonlinear Lorentzian fitting are also vital in determining the error bars.

4 Conclusions

In this paper, a DPAS technique was proposed to provide a precise frequency reference to experimentally determine the LIFS of the lowest vibrational levels of the molecular long-range state. The LIFS measurement of $\nu = 0$ and 1 supplemented the potential curve of the PLR state. Our scheme has several advantages. First, the LIFSs of the lowest vibrational levels of Cs_2 long-range states have been directly determined for the first time. Secondly, an onerous cavity is not required. Finally, this simple and robust scheme can be easily applied to investigate the potential behaviors of long-range states of other homonuclear or heteronuclear molecular species.

Acknowledgements This work was supported by the National Key R&D Program of China (Grant No. 2017YFA0304203), the National Natural Science Foundation of China (Grants Nos. 61722507,

61675121, and 61705123), PCSIRT (No. IRT-17R70), 111 Project (Grant No. D18001), the Program for the Outstanding Innovative Teams of Higher Learning Institutions of Shanxi (OIT), the Fund Program for the Scientific Activities of Selected Returned Overseas Professionals in Shanxi Province, and the Applied Basic Research Project of Shanxi Province, China (Grant Nos. 201701D221002, 201901D211191, and 201901D211188).

References

1. I. Bloch, J. Dalibard, and W. Zwerger, Many-body physics with ultracold gases, *Rev. Mod. Phys.* 80(3), 885 (2008)
2. J. Eisert, M. Friesdorf, and C. Gogolin, Quantum many-body systems out of equilibrium, *Nat. Phys.* 11(2), 124 (2015)
3. J. F. Barry, D. J. McCarron, E. B. Norrgard, M. H. Steinecker, and D. DeMille, Magneto-optical trapping of a diatomic molecule, *Nature* 512(7514), 286 (2014)
4. A. M. Rey, A. V. Gorshkov, C. V. Kraus, M. J. Martin, M. Bishof, M. D. Swallows, X. Zhang, C. Benko, J. Ye, N. D. Lemke, and A. D. Ludlow, Probing many-body interactions in an optical lattice clock, *Ann. Phys.* 340(1), 311 (2014)
5. J. L. Bohn, A. M. Rey, and J. Ye, Cold molecules: Progress in quantum engineering of chemistry and quantum matter, *Science* 357(6355), 1002 (2017)
6. N. Goldman, J. C. Budich, and P. Zoller, Topological quantum matter with ultracold gases in optical lattices, *Nat. Phys.* 12(7), 639 (2016)
7. K. M. Jones, E. Tiesinga, P. D. Lett, and P. S. Julienne, Ultracold photoassociation spectroscopy: Long-range molecules and atomic scattering, *Rev. Mod. Phys.* 78(2), 483 (2006)
8. C. Chin, R. Grimm, P. Julienne, and E. Tiesinga, Feshbach resonances in ultracold gases, *Rev. Mod. Phys.* 82(2), 1225 (2010)
9. N. V. Vitanov, A. A. Rangelov, B. W. Shore, and K. Bergmann, Stimulated Raman adiabatic passage in physics, chemistry, and beyond, *Rev. Mod. Phys.* 89(1), 015006 (2017)
10. L. Anderegg, B. L. Augenbraun, Y. Bao, S. Burchesky, L. W. Cheuk, W. Ketterle, and J. M. Doyle, Laser cooling of optically trapped molecules, *Nat. Phys.* 14(9), 890 (2018)
11. J. Rui, H. Yang, L. Liu, D. C. Zhang, Y. X. Liu, J. Nan, Y. A. Chen, B. Zhao, and J. W. Pan, Controlled state-to-state atom-exchange reaction in an ultracold atom–dimer mixture, *Nat. Phys.* 13(7), 699 (2017)
12. L. R. Liu, J. D. Hood, Y. Yu, J. T. Zhang, N. R. Hutzler, T. Rosenband, and K. K. Ni, Building one molecule from a reservoir of two atoms, *Science* 360(6391), 900 (2018)
13. W. B. Cairncross, D. N. Gresh, M. Grau, K. C. Cossel, T. S. Roussy, Y. Q. Ni, Y. Zhou, J. Ye, and E. A. Cornell, *Precision measurement of the electron's electric dipole moment using trapped molecular ions*, *Phys. Rev. Lett.* 119, 153001 (2017)
14. I. M. Georgescu, S. Ashhab, and F. Nori, Quantum simulation, *Rev. Mod. Phys.* 86(1), 153 (2014)
15. S. A. Moses, J. P. Covey, M. T. Miecnikowski, D. S. Jin, and J. Ye, New frontiers for quantum gases of polar molecules, *Nat. Phys.* 13(1), 13 (2017)
16. O. Dulieu and C. Gabbanini, The formation and interactions of cold and ultracold molecules: New challenges for interdisciplinary physics, *Rep. Prog. Phys.* 72, 086401 (2009)
17. D. Comparat, C. Drag, A. Fioretti, O. Dulieu, and P. Pillet, Photoassociative spectroscopy and formation of cold molecules in cold cesium vapor: Trap-loss spectrum versus ion spectrum, *J. Mol. Spectrosc.* 195(2), 229 (1999)
18. J. Ma, J. Wu, G. Chen, Q. Fan, H. Feng, X. Dai, W. Sun, L. Xiao, and S. Jia, Experimental determination of the rotational constants of high-lying vibrational levels of ultracold Cs_2 in the 0_g^- purely long-range state, *J. Phys. Chem. Lett.* 4(21), 3612 (2013)
19. S. Sainis, J. Sage, E. Tiesinga, S. Kotochigova, T. Bergeman, and D. DeMille, Detailed spectroscopy of the Cs_2 $a^3\Sigma+u$ state and implications for measurements sensitive to variation of the electron-proton mass ratio, *Phys. Rev. A* 86(2), 022513 (2012)
20. Y. Yang, X. Liu, Y. Zhao, L. Xiao, and S. Jia, Rovibrational dynamics of RbCs on its lowest $^{1,3}\Sigma^+$ potential curves calculated by coupled cluster method with all-electron basis set, *J. Phys. Chem. A* 116(46), 11101 (2012)
21. J. Wu, Z. Ji, Y. Zhang, L. Wang, Y. Zhao, J. Ma, L. Xiao, and S. Jia, High sensitive determination of light induced frequency shifts of ultracold cesium molecules, *Opt. Lett.* 36(11), 2038 (2011)
22. P. K. Molony, P. D. Gregory, Z. H. Ji, B. Lu, M. P. Köppinger, C. R. Le Sueur, C. L. Blackley, J. M. Hutson, and S. L. Cornish, Creation of ultracold $^{87}Rb^{133}Cs$ molecules in the rovibrational ground state, *Phys. Rev. Lett.* 113, 255301 (2014)
23. L. Lassablière and G. Quéméner, Controlling the scattering length of ultracold dipolar molecules, *Phys. Rev. Lett.* 121(16), 163402 (2018)
24. S. Ospelkaus, K. K. Ni, D. Wang, M. H. G. de Miranda, B. Neyenhuis, G. Quéméner, P. S. Julienne, J. L. Bohn, D. S. Jin, and J. Ye, Quantum-state controlled chemical reactions of ultracold Potassium-Rubidium molecules, *Science* 327(5967), 853 (2010)
25. M. Portier, S. Moal, J. Kim, M. Leduc, C. Cohen-Tannoudji, and O. Dulieu, Analysis of light-induced frequency shifts in the photoassociation of ultracold metastable helium atoms, *J. Phys. B* 39(19), S881 (2006)
26. I. D. Prodan, M. Pichler, M. Junker, R. G. Hulet, and J. L. Bohn, Intensity dependence of photoassociation in a quantum degenerate atomic gas, *Phys. Rev. Lett.* 91(8), 080402 (2003)
27. C. McKenzie, J. Hecker Denschlag, H. Häffner, A. Browaeys, L. E. E. de Araujo, F. K. Fatemi, K. M. Jones, J. E. Simsarian, D. Cho, A. Simoni, E. Tiesinga, P. S. Julienne, K. Helmerson, P. D. Lett, S. L. Rolston, and W. D. Phillips, Photoassociation of sodium in a bose-einstein condensate, *Phys. Rev. Lett.* 88(12), 120403 (2002)

28. A. Simoni, P. S. Julienne, E. Tiesinga, and C. J. Williams, Intensity effects in ultracold photoassociation line shapes, *Phys. Rev. A* 66(6), 063406 (2002)
29. J. L. Bohn and P. S. Julienne, Semianalytic theory of laser-assisted resonant cold collisions, *Phys. Rev. A* 60(1), 414 (1999)
30. Y. Q. Li, G. S. Feng, W. L. Liu, J. Z. Wu, J. Ma, L. T. Xiao, and S. T. Jia, Control of light induced frequency shift in ultracold cesium molecules by an external magnetic field, *Opt. Lett.* 40(10), 2241 (2015)
31. W. Liu, X. Wang, J. Wu, X. Su, S. Wang, V. B. Sovkov, J. Ma, L. Xiao, and S. Jia, Experimental observation and determination of the light induced frequency shift of hyperfine levels of ultracold polar molecules, *Phys. Rev. A* 96(2), 022504 (2017)
32. R. Wester, S. D. Kraft, M. Mudrich, M. Staudt, J. Lange, N. Vanhaecke, O. Dulieu, and M. Weidemüller, Photoassociation inside an optical dipole trap: Absolute rate coefficients and Franck–Condon factors, *Appl. Phys. B* 79(8), 993 (2004)
33. N. Bouloufa, A. Crubellier, and O. Dulieu, Reexamination of the 0_g^- pure long-range state of Cs_2: Prediction of missing levels in the photoassociation spectrum, *Phys. Rev. A* 75, 052501 (2007)
34. Y. Zhang, J. Ma, J. Wu, L. Wang, L. Xiao, and S. Jia, Experimental observation of the lowest levels in the photoassociation spectroscopy of the 0_g^- purely-long-range state of Cs_2, *Phys. Rev. A* 87, 030503 (2013)
35. J. Wu, W. Liu, Y. Li, J. Ma, L. Xiao, and S. Jia, Experimental determination of rotational constants of low-lying vibrational levels in the 0_g^- pure long-range state of ultracold Cs_2 molecule, *J. Quant. Spectrosc. Radiat. Transf.* 191, 13 (2017)
36. J. Wu, J. Ma, Y. Zhang, Y. Li, L. Wang, Y. Zhao, G. Chen, L. Xiao, and S. Jia, High sensitive trap loss spectroscopic detection of the lowest vibrational levels of ultracold molecules, *Phys. Chem. Chem. Phys.* 13(42), 18921 (2011)
37. M. Pichler, H. Chen, and W. C. Stwalley, Photoassociation spectroscopy of ultracold Cs below the $6P_{3/2}$ limit, *J. Chem. Phys.* 121(4), 1796 (2004)
38. A. Fioretti, D. Comparat, C. Drag, C. Amiot, O. Dulieu, F. Masnou-Seeuws, and P. Pillet, Photoassociative spectroscopy of the long-range state, *Eur Phys J. D* 5, 389 (1999)
39. M. Pichler, H. Chen, and W. C. Stwalley, Photoassociation spectroscopy of ultracold Cs below the $6P_{1/2}$ limit, *J. Chem. Phys.* 121(14), 6779 (2004)